



Article

Gardeniae Fructus Attenuates Thioacetamide-Induced Liver Fibrosis in Mice via Both AMPK/SIRT1/NF- κ B Pathway and Nrf2 Signaling

Mi-Rae Shin ¹, Jin A Lee ¹, Minju Kim ¹, Sehui Lee ¹, Minhyuck Oh ¹, Jimin Moon ², Joo-Won Nam ², Hyukjae Choi ^{2,3}, Yeun-Ja Mun ^{4,5} and Seong-Soo Roh ^{1,*}

¹ Department of Herbology, College of Korean Medicine, Daegu Haany University, Daegu 42158, Korea; with750@naver.com (M.-R.S.); tgs02022@naver.com (J.A.L.); mj8976@naver.com (M.K.); k18dw@naver.com (S.L.); gjo53@naver.com (M.O.)

² College of Pharmacy, Yeungnam University, Gyeongsan 38541, Korea; hyp1112@yu.ac.kr (J.M.); jwnam@yu.ac.kr (J.-W.N.); h5choi@yu.ac.kr (H.C.)

³ Research Institute of Cell Culture, Yeungnam University, Gyeongsan 38541, Korea

⁴ Department of Anatomy, School of Korean Medicine, Wonkwang University, Iksan 54538, Korea; yjmun@wku.ac.kr

⁵ Research Center of Traditional Korean Medicine, Wonkwang University, Iksan 54538, Korea

* Correspondence: ddede@dhu.ac.kr; Tel.: +82-53-770-2258



Citation: Shin, M.-R.; Lee, J.A.; Kim, M.; Lee, S.; Oh, M.; Moon, J.; Nam, J.-W.; Choi, H.; Mun, Y.-J.; Roh, S.-S. Gardeniae Fructus Attenuates Thioacetamide-Induced Liver Fibrosis in Mice via Both AMPK/SIRT1/NF- κ B Pathway and Nrf2 Signaling. *Antioxidants* **2021**, *10*, 1837. <https://doi.org/10.3390/antiox10111837>

Academic Editors:

Hyeong-Geug Kim and Gi-Sang Bae

Received: 22 October 2021

Accepted: 16 November 2021

Published: 19 November 2021

Publisher's Note: MDPI stays neutral with regard to jurisdictional claims in published maps and institutional affiliations.



Copyright: © 2021 by the authors. Licensee MDPI, Basel, Switzerland. This article is an open access article distributed under the terms and conditions of the Creative Commons Attribution (CC BY) license (<https://creativecommons.org/licenses/by/4.0/>).

Abstract: Liver fibrosis, which means a sort of the excessive accumulation of extracellular matrices (ECMs) components through the liver tissue, is considered as tissue repair or wound-healing status. This pathological stage potentially leads to cirrhosis, if not controlled, it progressively results in hepatocellular carcinoma. Herein, we investigated the pharmacological properties and underlying mechanisms of Gardeniae Fructus (GF) against thioacetamide (TAA)-induced liver fibrosis of mice model. GF not only attenuated hepatic tissue oxidation but also improved hepatic inflammation. We further confirmed that GF led to ameliorating liver fibrosis by ECMs degradations. Regarding the possible underlying mechanism of GF, we observed GF regulated epigenetic regulator, Sirtuin 1 (SIRT1), in TAA-injected liver tissue. These alterations were well supported by SIRT1 related signaling pathways through regulations of its downstream proteins including, AMP-activated protein kinase (AMPK), p47^{phox}, NADPH oxidase 2, nuclear factor erythroid 2-related factor 2 (Nrf2), and heme oxygenase-1, respectively. To validate the possible mechanism of GF, we used HepG2 cells with hydrogen peroxide treated oxidative stress and chronic exposure conditions via deteriorations of cellular SIRT1. Moreover, GF remarkably attenuated ECMs accumulations in transforming growth factor- β 1-induced LX-2 cells relying on the SIRT1 existence. Taken together, GF attenuated liver fibrosis through AMPK/SIRT1 pathway as well as Nrf2 signaling cascades. Therefore, GF could be a clinical remedy for liver fibrosis patients in the future.

Keywords: liver fibrosis; Gardeniae Fructus; thioacetamide; AMPK/SIRT1 pathway; Nrf2 signaling

1. Introduction

Liver fibrosis is provoked by chronic hepatic diseases and results from a disordered wound healing response [1]. The pathophysiological feature of liver fibrosis has mainly been characterized by the deposition of excessive extracellular matrix (ECM) molecules, particularly various collagen types. In addition, advanced liver fibrosis could lead to portal hypertension, hepatic dysfunction, liver cirrhosis, liver failure, and sometimes require liver transplantation [2]. For that reason, understanding the underlying mechanism, accurate diagnosis, and systematic approach in the early stages will accelerate its treatment and lessen the prevalence of cirrhosis. Hepatic stellate cells (HSCs) were reported as the fundamental collagen-producing cell in the liver since the 1980s [3]. Key signaling that regulates HSCs' fibrogenic actions was precisely described. Experimental animal models

for studying liver fibrogenesis were developed and led to the identification of key fibrogenic mediators [4]. To induce liver fibrosis, many chemical inducers such as thioacetamide, chloroform, iodoform, and carbon tetrachloride have been widely used. Chronic and persistent treatment using TAA induces liver injury, fibrosis, and finally cirrhosis derived from activation of HSCs [5,6]. Activated HSCs are alpha-smooth muscle actin (α -SMA)-positive cells that produce ECMs protein, including Collagen I [7]. Therefore, various studies to investigate target factors of activated HSCs were considered as crucial progress in a reversal of liver fibrosis [8].

Gardeniae Fructus (GF, the dried ripe fruits of *Gardenia jasminoides* Ellis) not only has been popularly applied to traditional medicine to treat hepatic disorders or to decrease various inflammation but also epidemically used as an excellent natural colorant. A total of 162 components have been separated and identified from GF [9]. Among the various compounds from GF, geniposide is one of the most important iridoid compounds and it was validated the pharmacological properties including anti-oxidative, anti-inflammatory, hepatoprotective, anti-depressive, anxiolytic activities, and beneficial effects on cardiovascular and digestive systems either in vitro or in vivo [10,11].

On the other hand, Silymarin, which is used as a positive control in this experiment, is distributed in the fruit and seeds of milk thistle. Silymarin exerts the hepatoprotective effects from inflammation, oxidative stress, and consequent cytotoxicity in patients with fibrosis or cirrhosis without serious adverse events [12].

In the current study, as purposed to investigate the pharmacological properties of GF against TAA (i.p.) to induce liver fibrosis of mice model, and our data elucidated new knowledge about anti-hepatofibrotic effects of GF. Additionally, we also provide the possible mechanisms GF which could mainly affect AMPK/SIRT1 pathway and/or Nrf2 signaling cascades on the liver fibrosis as well as chronic TAA exposure hepatic oxidative stress conditions.

2. Materials and Methods

2.1. Materials

Sodium carbonate (Cat No. 222321), quercetin (Cat No. Q4950), dimethyl sulfoxide (DMSO, D2650), silymarin (Cat No, S0292), and thioacetamide (Cat No. 163678) were provided by Sigma Aldrich Co. (St Louis, MO, USA). L-ascorbic acid was provided by Alfa Aesar (Cat No. A15613, Lancashire, UK).

2.2. Preparation of the Plant Material and Finger Printing Analysis of GF

The GF used in this experiment was a medicinal herb produced in Goheung, Jellannam-do in 2019, and was supplied from Bonchowon (Yeongcheon, Gyeongsanbuk-do). Dried GF (100 g) boiled with water (1 L) at 25 °C for 2 h. The powder of GF was a yield of 24.6% by weight and kept at −80 °C before use. GF power (1 mg) was dissolved in 2 mL of 100% methanol. The solution was centrifuged at 13,500 rpm for 3 min and the supernatant was collected for component analysis. We injected 3 μ L of the sample into a Waters Acquity UPLC system (Waters®, Milford, MA, USA) using a reversed-phase C18 column (Phenomenex HPLC part: Luna 3 μ C18(2) 100 Å, 150 mm \times 4.6, Torrance, CA, USA). The mobile phase composition was as follows: solvent A (5% acetonitrile in deionized water with 0.05% formic acid), solvent B (100% acetonitrile with 0.05% formic acid). The gradient conditions; A:B = 90:10 (0 min) \rightarrow 90:10 (2 min) \rightarrow 80:20 (3 min) \rightarrow 80:20 (6 min) \rightarrow 0:100 (8 min) \rightarrow 0:100 (10 min) \rightarrow 90:10 (11 min) \rightarrow 90:10 (14 min). The flow rate was 0.7 mL/min with UV absorption monitoring at 254 nm. The peak of geniposide was assigned by comparison of retention time and UV spectrum of authentic standard. Geniposide was detected as a major compound from the chromatogram of the extract. Representative UPLC chromatogram was illustrated in Supplementary Figure S1A–D. Quantification of geniposide in the extract was performed by peak area measurement. The calibration curve of geniposide was made at the concentration of 6.25, 12.5, 25, 50, 100,

200, and 400 µg/mL with an injection volume of 3 µL each and the replication of five. The regression coefficient (R^2) was calculated as 0.9994 (standard curve; $y = 4.3285x - 8.4191$).

2.3. Mice Treatment

The animal protocol was approved by the Ethics Committee of the Daegu Haany University and performed according to 'the Guidelines for Animal Experiment'. C57BL/6 mice (male, 20–25 g) were purchased from DBL (Eumseong, Korea). The mice were maintained at 22 ± 2 °C and controlled with a 12 h light/dark cycle and humidity ($50 \pm 5\%$). After 1 week of adaptation, a total of thirty-six mice were divided into 4 groups ($n = 9$ for each group): Normal, Control (TAA only), GF (200 mg/kg), and Silymarin (50 mg/kg), respectively. Mice in the normal group were intraperitoneally injected 0.9% normal saline orally administrated with distilled water (DW); the control group received TAA (i.p.) and DW (peroral, p.o.); the Silymarin group received TAA (i.p.) and Silymarin at 50 mg/kg/day (p.o.); the GF group received TAA (i.p.) and GF at 200 mg/kg/day (p.o.) for 8 weeks of experimental periods (Supplementary Figure S2).

Liver fibrosis was induced by TAA three times injection per week for 8 weeks according to an escalating treatment dose protocol (100 mg/kg for 1st week; 200 mg/kg for from 2nd to 3rd week, and 400 mg/kg for 4th to 8th week, respectively). The treatment drugs for liver fibrosis both GF (200 mg/kg/day) and Silymarin (50 mg/kg/day) were continuously administrated for 8 weeks 90 min prior to TAA injection. On the final day of the experiment, whole blood samples were collected from the abdominal vein and centrifuged at 4000 rpm for 10 min (at 4 °C), then stored in -80 °C freezer for further analyses. Liver tissues were removed immediately transferred 10% neutral formalin for the purpose of histological analysis and liquid nitrogen gas then stored at -80 °C for further biochemistry analysis, respectively.

2.4. Histological Examination

Liver tissue samples were fixed in 10% formalin then processed for embedding and sectioning at the Kyeongbook National University Hospital BMRI (Daegu, Korea). Liver sections (3 µm thickness) were stained using hematoxylin and eosin (H&E), Masson's trichrome (MT), and Sirius Red staining which were followed by the standard protocol. The images were captured using Olympus BX51 Microscope (Olympus Co., Ltd., Tokyo, Japan, 40-, 100-, and 200- \times magnifications) and then analyzed using the I-Solution Lite software program (IMTechnology, Vancouver, BC, Canada).

2.5. Analysis of Serum Biochemistry

Liver enzymes such as aspartate aminotransferase (AST) and alanine aminotransferase (ALT) were measured by serum levels using a Transaminase CII-Test (Wako Pure Chemical Industries Ltd., Osaka, Japan). Serum ammonia was measured by ELISA kit (Abcam, Cambridge, UK) according to the manufacturer's instructions.

2.6. Analysis of Immunohistochemistry (IHC) and Immunofluorescence (IF)

IHC analysis was performed for detecting Kupffer cells (F4/80), bile duct cells (CK-19), and Collagen type 3. We further completed IF analyses for observing 4-HNE, desmin, α -smooth muscle actin (α -SMA), and Collagen type 1, respectively (Supplementary Figure S7). Briefly, paraffin embedding liver tissue sections were deparaffinized and rehydrated with various gradations of ethanol. After washing with liver sections with tap water, they were progressed to peroxidase removal with 5% hydrogen peroxide in absolute methanol for 5 min. Tissues were incubated in 2.5% normal horse serum (NHS) then applied primary antibodies for overnight at 4 °C. Tissue sections were washed applied horseradish peroxidase (HRP)-conjugated secondary antibodies, then applied the signals using 3-Amino-9-ethyl carbazol (AEC) and mounted with mounting buffer. The images of IHC analysis were captured using light microscopy conditions (Olympus BX51, Tokyo, Japan, 100- and 400- \times) and IF images were observed by fluorescent filters equipped microscope (Carl Zeiss, Ger-

many, 100- and 200- \times). The quantification analysis of each positive signal for IHC or IF image was obtained from the randomly selected sections of at least four fields of each sample using Image J 1.52 software (NIH, Bethesda, MD, USA).

2.7. Measurement of Myeloperoxidase (MPO) and TBA-Reactive Substance (TBARS) Levels

MPO in serum was determined via a colorimetric kit of BioVision, Inc. (Milpitas, CA, USA). TBARS assay to evaluate malondialdehyde (MDA) was estimated according to the method of Mihara and Uchiyama [13].

2.8. Cell Cultures

For validating possible mechanisms of GF on hepatic oxidation and fibrosis we cultured human blastoma cell line, HepG2, and hepatic stellate cells (HSCs) line, LX-2 cells, respectively. HepG2 cells were cultured in 10% fetal bovine serum (FBS) containing DMEM, and LX-2 cells were cultured 5% FBS contained DMEM under the condition of 5% CO₂ supplementary with 37 °C incubators, respectively.

For hepatic oxidative stress condition, we treated 500 μ M of hydrogen peroxide (H₂O₂) during 6- and 24-h after pre-treatment with 50, 100, and 200 μ g/mL of GF, then cells were washed with 10 mM PBS (pH 7.3) twice and fixed in 4% paraformaldehyde (PFA) or cell lysis buffers (for Western blot analysis) according to each specific experimental condition.

For liver fibrosis condition, we active LX-2 cells by transforming growth factor (TGF)- β 1 (10 ng/mL) for 18 h incubation after pre-treatment with GF (200 μ g/mL) for 6 h and followed to the washing and fixing for further analysis, respectively. IHC or IF analysis using HepG2 cells or LX-2 cells, we used standard protocol. Briefly, the cells were washed with PBS (10 mM, pH 7.3) twice and fixed in 4% paraformaldehyde for 1 h at RT. Cells were washed with PBS twice and incubated with 0.3% Triton X-100 for 5 min at RT, then underwent PBS washing twice. Cells were treated 2.5% NHS which is known as blocking buffer for 1 h at RT and primary antibodies were treated then incubated at 4 °C overnight. After washing with PBS three times (each time for 10 min) at RT, we treated fluorescent conjugated secondary antibodies for IF analysis or HRP-conjugated secondary antibody for IHC, respectively.

For IF analysis, we followed the further washing steps using twice PBS and one 0.05% PBST for 10 min, and IHC analysis we washed with PBS three times using PBS, respectively. After washing secondary antibodies for each experiment, the positive signals were detected by the development of AEC and performed counterstaining using hematoxylin. In the case of IF analysis, we completed the counterstaining by application of DAPI solution to the cells.

Images were captured according to each experiment type as followed by the liver tissue sections.

2.9. Western Blotting

To obtain cell samples, we used the lysis buffer was composed of various compounds as follows; 50 mM Hepes, pH 7.5, 150 mM NaCl, 10% glycerol, 1% Triton X-100, 1.5 mM MgCl₂, 1 mM EGTA, 10 mM sodium pyrophosphate, 100 mM sodium fluoride, and freshly added 100 μ M sodium vanadate, 1 mM PMSF, 10 μ g/mL aprotinin, and 10 μ g/mL leupeptin, respectively or NP-40 lysis buffer (1% NP-40, 20 mM Tris, pH 7.4, 137 mM NaCl, 2 mM EDTA, 10% glycerol, 1 mM PMSF, and 1 \times cOmplete™ protease inhibitor cocktail). For cytochrome c, COX IV, and GAPDH in either cytosolic or mitochondrial fraction, we obtained each fractionated sample using a commercially available kit (Mitochondria/Cytosol Fractionation Kit, BioVision, Catalog #K256-25, Milpitas, CA, USA).

To obtain cytosol samples of tissue, liver tissues were lysed with buffer consisting of follows; 0.1 mM EDTA, 10 mM HEPES (pH 7.8), 0.1 mM PMSF, 10 mM KCl, 1 mM DTT, 2 mM MgCl₂, and 1250 μ L protease inhibitor solution (Wako, Osaka, Japan). The homogenates were incubated (4 °C for 20 min), and then 10% NP-40, respectively. After centrifugation with the above lysis buffer (12,000 rpm at 4 °C for 2 min, Eppendorf 5415R,

Hamburg, Germany). Then the supernatant was collected as a cytosol sample, and the lysates were suspended with 20 mL ice-cold lysis buffer for intending to extract nucleus (50 mM HEPES (pH 7.8), 50 mM KCl, 300 mM NaCl, 1 mM DTT, 0.1 mM EDTA, 1% (*v/v*) glycerol, 0.1 mM PMSF, and 100 μ L protease inhibitor solution, respectively) and suspended and incubated (4 °C for 30 min), then performed centrifugation (12,000 rpm at 4 °C for 10 min). The supernatant was finally collected as a nuclear sample. Both cytosol and nuclear samples were stored at -80 °C for further experiments.

Samples containing 10–12 μ g of protein were electrophoresed through 8–15% SDS-PAGE and transferred to a nitrocellulose membrane. Each membrane was blocked with 5% (*w/v*) skim milk solution for 1 h and visualized using ECL reagents of GE Healthcare (Chicago, IL, USA). The bands were detected by Sensi-Q 2000 Chemidoc (Lugen Sci Co., Ltd., Gyeonggi-do, Bucheon-si, Korea). Antibodies used in western blotting are shown in Supplementary Figure S8. We followed the methods of Mi-Rae Shin et al. [14].

The quantification analysis of each band was analyzed by application of Image J 1.52 software (NIH, Bethesda, MD, USA).

2.10. Statistical Analysis

All statistical data were expressed as mean \pm SEM through the present manuscript by the performance of the Prism 9.2 software from GraphPad (La Jolla, CA, USA). Comparisons between two groups were performed using a two-tailed unpaired Student *t*-test. Comparisons for more than two groups, we performed one-way or two-way ANOVA followed by Tukey's post-hoc tests.

3. Results

3.1. GF Attenuated TAA-Mediated Chronic Liver Injury

TAA injection considerably decreased BW as compared with the normal group, and there were no significant differences among the control, GF 200, and Sily 50 groups during experiment periods. ($p < 0.001$ for time-dependent manners of BW changes and among the groups, Figure 1A). The final BW and liver WT were significantly reduced by TAA injection in the control group as compared with the normal group ($p < 0.001$ or 0.05 in Figure 1B,C), and both drug treatment groups didn't show a significance as compared with the control group (Figure 1B,C). Relative liver mass was significantly increased by TAA injection in the control group as compared with the normal group ($p < 0.001$), whereas GF 200 significantly decreased relative liver tissue mass as compared with the control group, but not Sily 50 ($p < 0.05$, Figure 1D). Eight weeks of TAA injection severely led to liver damage by evidence of histopathological alterations based on the H&E staining. As compared to the normal group, the control group showed infiltrations of inflamed cells and hepatocyte cell deaths through the liver tissue (Figure 1E). Additionally, liver enzymes such as serum AST and ALT levels in the control group were significantly increased as compared with the normal group, respectively (Figure 1F,G). These liver injuries were well represented by abnormal elevations of serum ammonia levels in the control group (Figure 1H). Administration with GF during entire experimental periods expected not only attenuated liver inflamed cell infiltrations with hepatocyte deaths by histological inspection, but also significantly exerted to decrease serum AST, ALT, and ammonia levels, respectively ($p < 0.01$ for AST, $p < 0.05$ for ALT, and $p < 0.001$ for ammonia, Figure 1F–H). TAA induced hepatic tissue injuries were not only improved histopathological examinations in Sily 50 group (Figure 1E), but also significantly attenuated by features of serum biochemistries and serum ammonia levels (Figure 1F–H); however, silymarin 50 mg/kg treatment didn't significantly alter general outcomes in the present study.

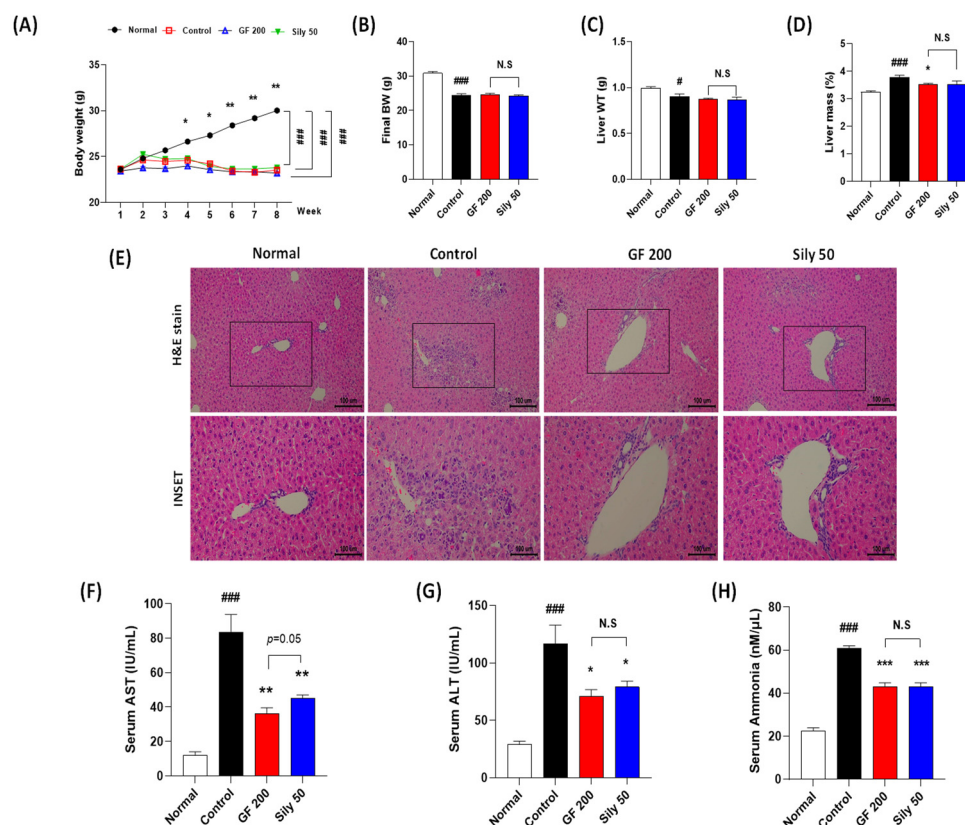


Figure 1. Effects of GF on the TAA-injected liver fibrosis of mice model. General outcomes for (A) body weight changes, (B) final body weight, (C) liver tissue weights, and (D) relative liver weights. (E) Histopathological examinations of H&E stain. (F) Serum AST, (G) ALT, and (H) ammonia levels. Data were expressed mean \pm SEM ($n = 9$ for each group). N.S, not significant, # $p < 0.05$ and ### $p < 0.001$ for Normal vs. Control; * $p < 0.05$, ** $p < 0.01$, and *** $p < 0.001$ for Control vs. GF 200 or Sily 50. H&E staining images were captured by light microscope condition (100- or 400- \times magnifications).

Compared to the pharmacological properties between GF 200 and Sily 50, there was a tendency that GF 200 seemed better in serum AST and ALT levels than Sily 50, but other factors were shown similar effects.

3.2. Effects of GF on TAA-Induced Hepatic Tissue Oxidation

Next, we addressed that the TAA-induced hepatic injury in the present study by focusing on the oxidative stress and antioxidant components alterations. First, we measured IF analysis against 4-HNE which is a correlation marker of final oxidative stress product ($p < 0.001$). As expected, the control group significantly increased the positive signals of 4-HNE as compared with the normal group. Additionally, serum MPO activities in the control group were significantly increased as compared with the normal group ($p < 0.001$). This pathological alteration was well supported by abnormal oxidative stress status in both serum and hepatic protein levels of MDA, which is a marker of lipid peroxidation ($p < 0.01$, Figure 2D,E), whereas administration with GF 200 mg/kg significantly ameliorated the above pathological statuses ($p < 0.001$ for 4-HNE IF analysis, $p < 0.01$ for MPO and hepatic MDA, and $p < 0.05$ for serum MDA, Figure 2A–E). Western blot analysis well displayed that the hepatic antioxidants such as GPx-1/2 and SOD were significantly deterred by 8 weeks of TAA injection in the control group ($p < 0.001$ or 0.01), whereas GF 200 significantly prevented from deterioration of two major antioxidant enzymes in the hepatic tissue against TAA mediated-hepatic tissue oxidation ($p < 0.05$ or 0.01 in Figure 2F,G).

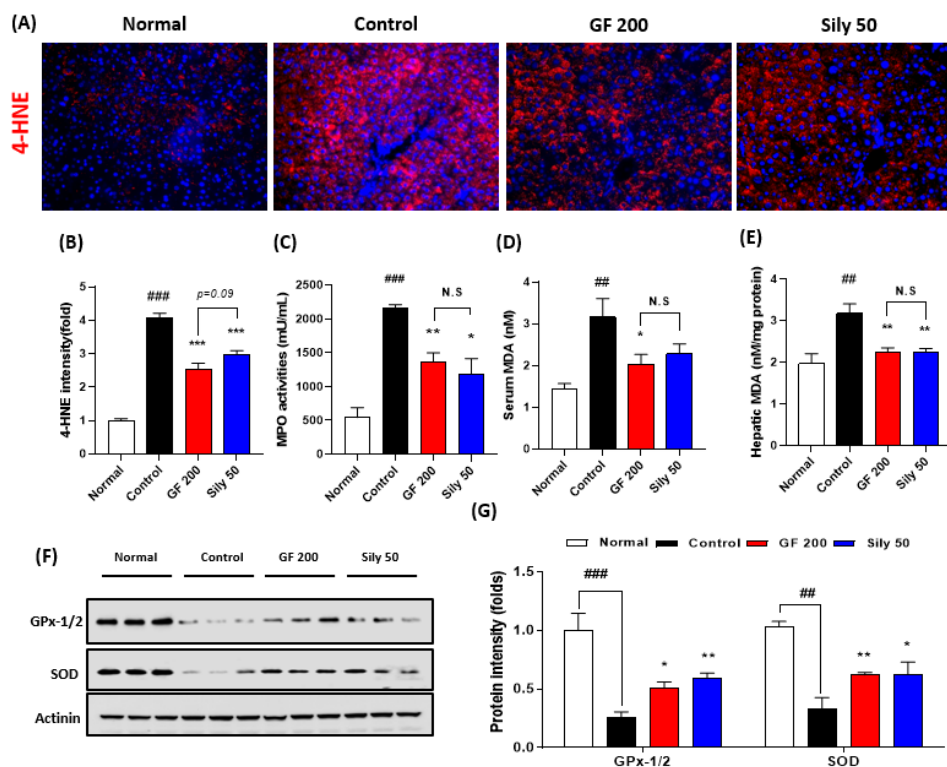


Figure 2. Antioxidant effects of GF on the TAA-induced hepatic tissue oxidation. (A) IF analysis against 4-HNE and (B) quantification analysis. (C) MPO activities in the serum level. (D) Serum MDA and (E) hepatic MDA levels. (F) Western blot analysis of GPx-1/2 and SOD in hepatic protein levels. (G) Quantification analysis of GPx-1/2 and SOD. Data were expressed mean \pm SEM ($n = 9$ for each group). N.S, not significant, $\#\# p < 0.01$ and $\#\#\# p < 0.001$ for Normal vs. Control; $* p < 0.05$, $** p < 0.01$, and $*** p < 0.001$ for Control vs. GF 200 or Sily 50. Images were captured by fluorescence filter equipped with microscope condition (100- or 400- \times magnifications).

Sily 50 group exhibited similar efficacies of GF 200 as compared with the control group against hepatic oxidations ($p < 0.05$, 0.01, or 0.001, Figure 2A–G).

3.3. Effects of GF on Hepatic Inflammation

Hepatic inflammation is one of the representative pathological phenotypes of TAA-induced hepatic injury. Thus, we examined the pharmacological properties of GF focusing on the inflammatory reaction-related markers. We presented IHC against F4/80 which is a marker of Kupffer cells in the liver tissue resided macrophage. As we expected, the positive signals were remarkably enhanced in the control group as compared with the normal group ($p < 0.001$), while GF 200 significantly attenuated these positive signals as compared with the control group ($p < 0.05$ in Figure 3A,B). Pro-inflammatory cytokines such as IL-1 β and TNF- α in hepatic protein levels of the control groups were considerably increased in the response to TAA-induced hepatic injury ($p < 0.01$); however, administration with GF 200 mg/kg exerted to decrease these pro-inflammatory cytokines as compared with the control group ($p < 0.05$ or 0.01 in Figure 3C,D). To elucidate the pharmacological properties of GF 200 focusing on the possible molecular signaling pathways of hepatic inflammation, we performed Western blot analysis against NF- κ B, I κ B α , iNOS, and p38 with their phosphorylated forms in hepatic protein levels, all targeted proteins in the control group were drastically altered according to our expectation as compared to the normal group ($p < 0.001$); however, we also observed that GF 200 mostly normalized the above inflammatory target proteins' abnormalities with statistical significance as compared with the control group ($p < 0.01$, or 0.001 in Figure 3E,F).

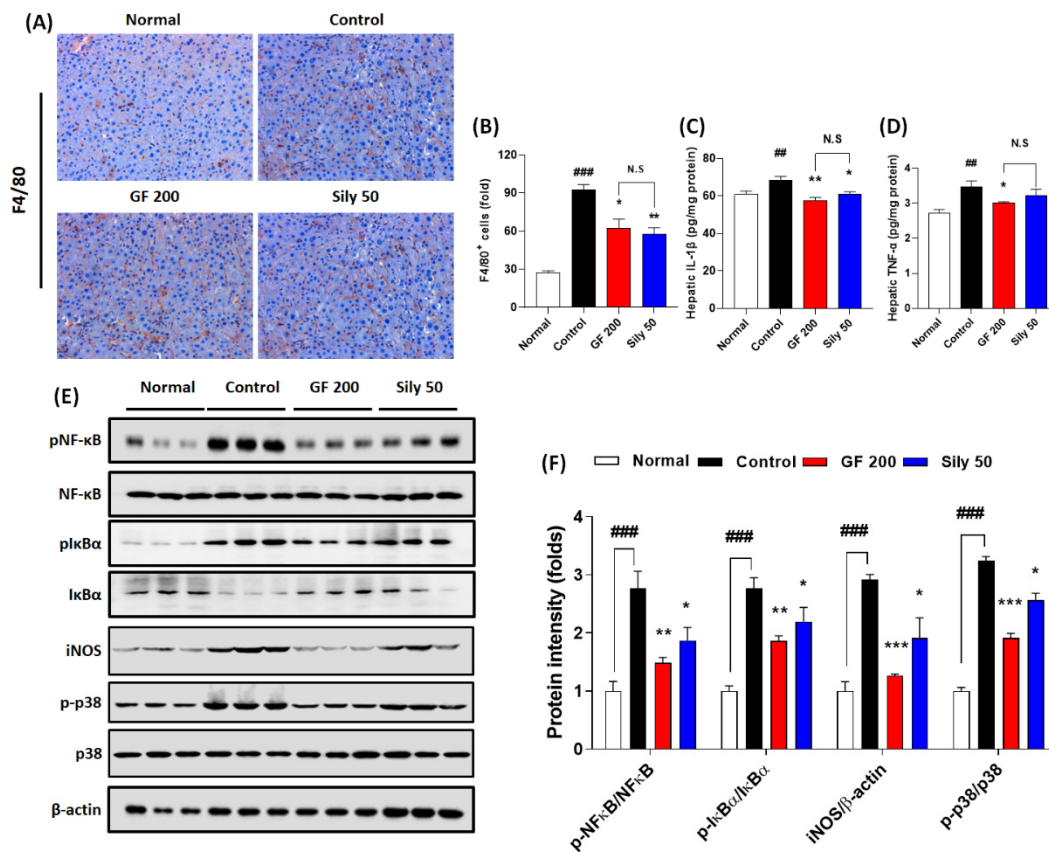


Figure 3. Effects of GF on TAA-injected hepatic inflammation. (A) IHC analysis against F4/80 and (B) quantification analysis. (C) Hepatic protein levels of IL-1 β and (D) TNF- α . (E) Western blot analysis of inflammatory related proteins including p-NF- κ B, NF- κ B, p-I κ B α , I κ B α , iNOS, p-p38, and p38 and (F) protein intensity. Data were expressed mean \pm SEM ($n = 4$ for each group in IHC analysis; $n = 9$ for each group for IL-1 β and TNF- α ; $n = 3$ for each group in Western blot analysis). N.S, not significant, $^{##} p < 0.01$ and $^{###} p < 0.001$ for Normal vs. Control; $^* p < 0.05$, $^{**} p < 0.01$, and $^{***} p < 0.001$ for Control vs. GF 200 or Sily 50. H&E staining images were captured by light microscope condition (400- \times magnifications).

Administration with Silymarin 50 mg/kg showed beneficial effects on F4/80 IHC analysis ($p < 0.01$), hepatic protein levels of IL-1 β ($p < 0.05$), and phosphorylated forms of NF- κ B, I κ B α , and p38 and iNOS protein levels which were evidenced by Western blot analysis ($p < 0.05$ for Figure 3E,F).

3.4. Effects of GF on the Hepatic Fibrosis

Next, we further examined the pharmacological effects of GF on hepatic fibrosis. Both Masson's trichrome and Sirius Red stains well evidenced that TAA-induced liver fibrosis by huge amount collagen deposition through hepatic tissue (positive color for blue in Masson's trichrome and red color for Sirius Red staining) in the control group as compared with the normal group ($p < 0.001$). Representative ECMs molecules of IF or IHC against α -SMA, Collagen type 1, and Collagen type 3 were also abnormally enhanced through liver tissue by TAA injection ($p < 0.001$). These alterations, as our expectation, were significantly resolved in the GF 200 group as compared to the control group ($p < 0.01$ in Figure 4A–J). These alterations were well correlated with the numbers of HSCs in the liver tissue which were by the performance of IF analysis against Desmin. Desmin positive signals (part of red fluorescence) were remarkably enhanced in the control group as compared with the normal group, but these signals were drastically decreased as compared with the control group (Supplementary Figure S3). Additionally, the representative profibrogenic cytokine and ECMs-related target proteins including TGF- β 1, TIMP-1, MMP-1, and MMP-13 in the hepatic protein levels were abnormally altered in the control group as compared with the

normal group ($p < 0.05$, 0.01 , or 0.001 , respectively). Administration with GF 200 mg/kg not only significantly led to a decrease in TGF- β 1 and TIMP-1, but also increase MMP-1 and MMP-13 as compared to the control group ($p < 0.05$ or 0.01 in Figure 4K,L). Interestingly, we also examined the ductular reactions of bile duct area through the liver tissue, but there were no significant features, only the number of bile duct area were increased in the control group as compared with the normal group. In addition, no differences were not observed between GF 200 and Sily 50 as compared with the control group by evidence of IHC analysis against CK-19 (Supplementary Figure S4).

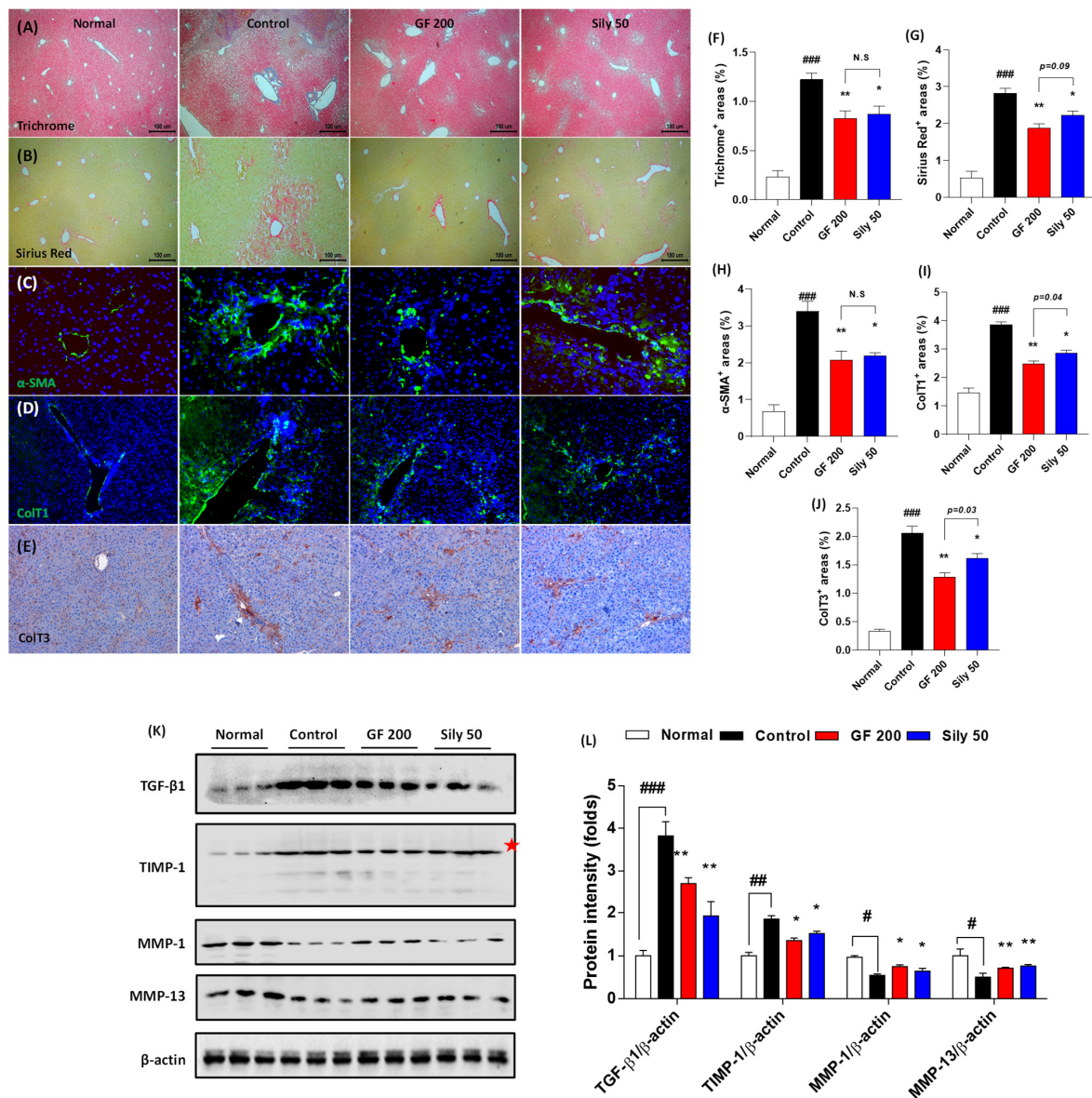


Figure 4. GF attenuates liver fibrosis by degradations of ECMs in tissue. (A) Masson’s trichrome staining, (B) Sirius Red staining, (C) IF analysis against α -SMA, (D) Collagen type 1, and (E) IHC against Collagen type 3. (F–J) Quantification analyses for Masson’s trichrome staining, Sirius Red staining, IF analysis against α -SMA, Collagen type 1, and IHC against Collagen type 3. (K) Western blot analysis of ECM proteins TGF- β 1, TIMP-1, MMP-1, and MMP-13 and (L) protein intensity. Data were expressed mean \pm SEM ($n = 4$ for each group in staining images; $n = 3$ for each group for Western blot analysis). N.S, not significant, # $p < 0.05$, ## $p < 0.01$, and ### $p < 0.001$ for Normal vs. Control; * $p < 0.05$ and ** $p < 0.01$ for Control vs. GF 200 or Sily 50. Masson’s trichrome, Sirius Red staining, and IHC against Collagen type 3 images were captured by light microscope condition (40-, 100-, and 200- \times magnifications). IF images were observed by fluorescence filtered equipped microscopy condition (200- \times magnifications).

The positive control group, Sily 50, showed similar properties on the liver fibrosis by amelioration collagen accumulation as well as exertion of fibrogenic cytokine and ECMs-related proteins ($p < 0.05$ or 0.01). The number of HSCs through the liver tissue was diminished in Sily 50 as compared with the control group (Supplementary Figure S3), but Sily 50 didn't alter ductular reactions (Supplementary Figure S4).

3.5. Pharmacological Properties of GF against TAA-Induced Hepatic Fibrosis via Modulations of SIRT1

To validate the possible underlying mechanism of GF on TAA-injected hepatic fibrosis, we focused on the epigenetic regulator, SIRT1 which is well known for a NAD^+ , NADH-dependent class III protein deacetylase-enzyme. Our Western blot analysis results well evidenced that SIRT1 in hepatic protein levels of the control group was considerably depleted as compared with the normal group ($p < 0.001$), and H3K9Ac also well support the above alterations in hepatic protein levels of TAA-injected liver tissue by drastically increase manners compared to the normal group ($p < 0.001$). Administration with GF 200 mg/kg significantly normalized against these alterations in hepatic protein levels as compared with the control group ($p < 0.01$ for SIRT1 and H3K9Ac). Additionally, the up-streaming molecule of AMPK α , which is a p-LKB1 was significantly decreased in the control group as compared with the normal group, the GF significantly increased p-LKB1 as compared with the control group ($p < 0.05$). Regarding the molecular levels of the relationship between SIRT1 and AMPK α , we observed that AMPK α was drastically activated by the deterioration of SIRT1 ($p < 0.05$). We further observed that SIRT1 target oxidative stress-related proteins such as NOX2 and p47^{phox} were significantly normalized by GF 200 against TAA-injected hepatic fibrosis ($p < 0.05$ or 0.01). Additionally, AMPK α targeted proteins which are NADPH activity relying on antioxidant enzymes Nrf2 and HO-1 were also deterred by TAA and remarkably recovered by GF 200 mg/kg ($p < 0.01$, Figure 5A–C).

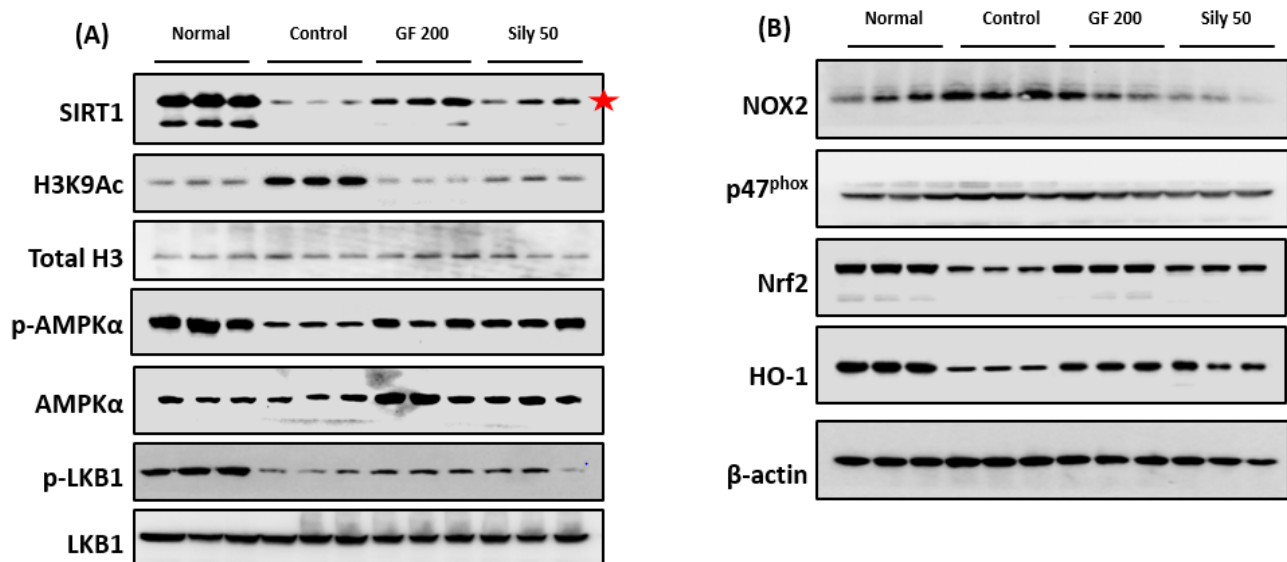


Figure 5. Cont.

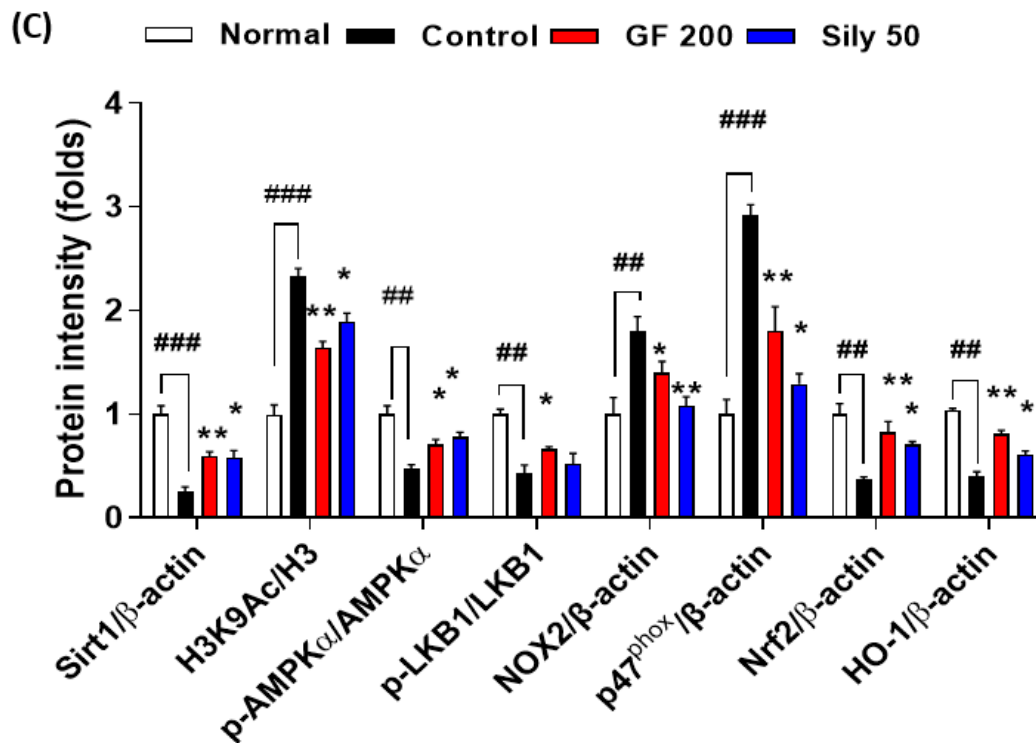


Figure 5. GF ameliorates liver fibrosis via regulations of AMPK/SIRT1 signaling pathways. Western blot analysis of SIRT1 and its deacetylase target proteins such as H3K9Ac, Total H3, p-AMPK α , and AMPK α , p-LKB1, and LKB1 (A), and NOX2, p47^{phox}, Nrf2, and HO-1 (B). (C) Quantification analysis of Western blot analysis. Data were expressed mean \pm SEM ($n = 3$ for each group for Western blot analysis). ## $p < 0.01$ and ### $p < 0.001$ for Normal vs. Control; * $p < 0.05$ and ** $p < 0.01$ for Control vs. GF 200 or Sily 50.

As a positive drug treatments Silymarin 50 mg/kg, also well showed beneficial properties on TAA-induced liver fibrosis by controlling of SIRT1 / AMPK α signaling pathways with statistical significances as compared with the control group ($p < 0.01$, Figure 5A–C).

3.6. GF Prevents Hepatocyte Oxidation by Increase of SIRT1 in Time Dependent Manners

To explain the pharmacological mechanisms of GF 200 on oxidative stress-induced hepatocyte damage, we explored hydrogen peroxide (H₂O₂)-induced hepatocyte oxidation using HepG2 cells which is a human blastoma cell line. First, we intended to confirm the alterations of SIRT1 would be affected by time-dependent manner or not. Interestingly, we observed that chronic exposure of H₂O₂ (500 μ M incubation for 24 h, Figure 6B) in the HepG2 cells were considerably depleted SIRT1 in the protein levels as compared with the control group, but not acute exposure (6 h, Figure 6A). As expected, we also confirmed that chronic exposures to H₂O₂ could significantly enhance dead cell numbers ($p < 0.001$, Supplementary Figure S5A,B), which were well supported by abnormal releases of cytochrome *c* from mitochondria to cytosolic levels by evidence of Western blot analysis (Supplementary Figure S5C,D). To verify oxidative stress is a deciding factor by SIRT1 existence or not, we further performed IHC analysis against 4-HNE and SIRT1 after 24 h of H₂O₂ incubated cells. 4-HNE positive signals were also hugely enhanced in H₂O₂ group as compared with the normal group ($p < 0.001$ in Figure 6C,E), which were reversely appeared in the positive signals of SIRT1 in the drug-treated groups ($p < 0.001$ in Figure 6D,F), respectively.

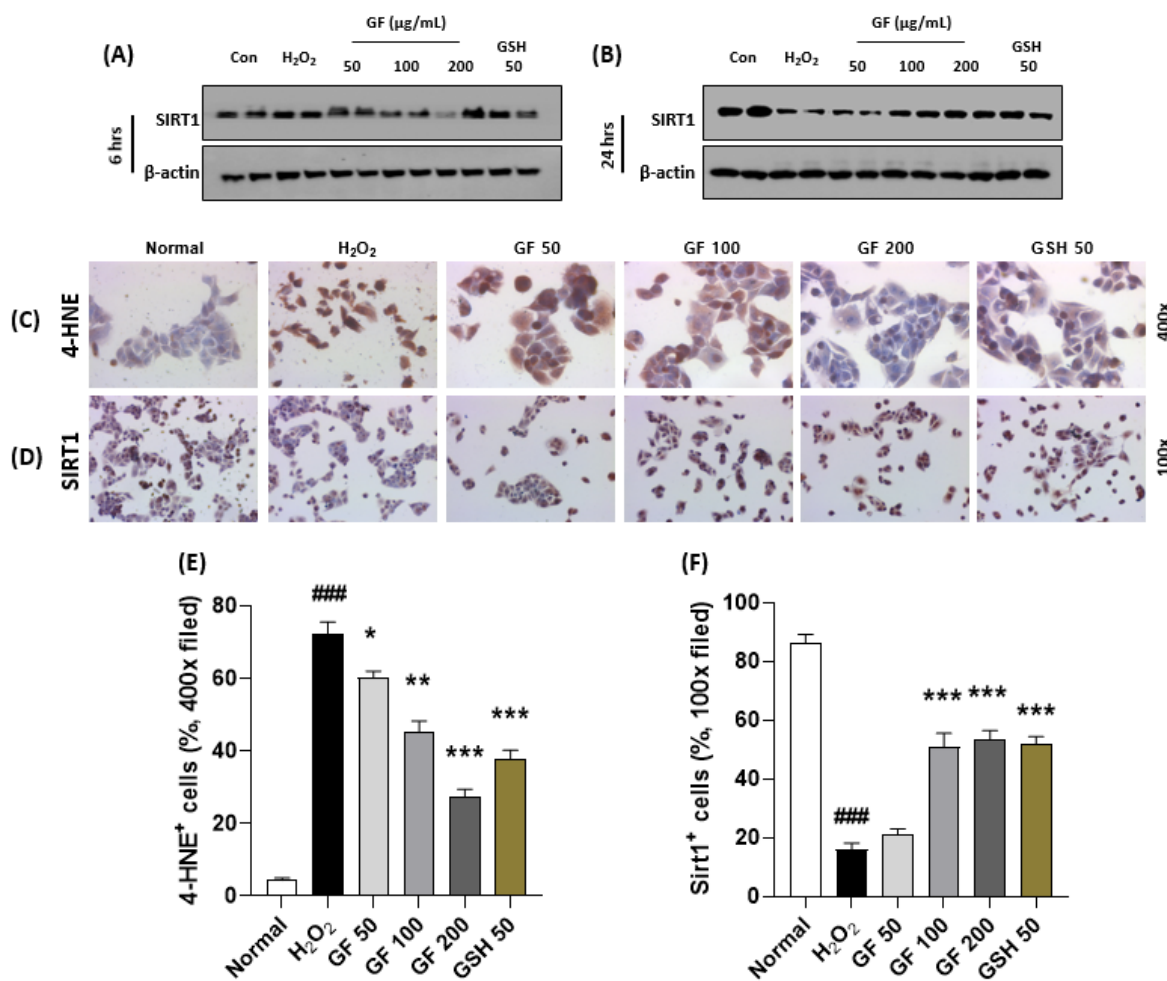


Figure 6. GF attenuates hepatocyte oxidative stress via prevention from SIRT1 depletions. Western blot analysis in H₂O₂ (500 μM) treated HepG2 cells for 6 h or 24 h with or without GF (50, 100, 200 μg/mL). Cellular protein levels of SIRT1 for 6 h (A) and 24 h (B). IHC analysis against 4-HNE (C) and SIRT1 (D). Quantification analysis of 4-HNE (E) and SIRT1 (F). Data were expressed mean ± SEM ($n = 4$ for IHC analysis). ### $p < 0.001$ for Normal vs. H₂O₂ and * $p < 0.05$, ** $p < 0.01$, and *** $p < 0.001$ for H₂O₂ vs. GF or GSH. IHC images were captured by microscope condition (100- or 400- \times magnifications).

Pre-treatment with GF with various doses (6 h prior to hydrogen peroxide with 50, 100, and 200 μg/mL) significantly prevented the depletion of SIRT1 in cellular protein levels of the chronic exposure condition ($p < 0.001$ for Figure 6B,D,F). According to these properties, GF could block oxidative stress as well as cell death which were well evidenced by 4-HNE ($p < 0.001$ for Figure 6C,E), LIVE/DEAD cell ($p < 0.001$ for Supplementary Figure S5A,B), Western blot analysis of cytochrome *c* in mitochondria and cytosolic levels (Supplementary Figure S5C,D).

3.7. GF Promotes Inactivation of TGF-β1 Incubated Culture-Induced Activated HSCs by Prevention of SIRT1

To validate the underlying mechanisms of GF against liver fibrosis, we performed TGF-β1 treated LX-2 cell activation in vitro experiment. As our expectation, TGF-β1 considerably decreased cellular protein levels of SIRT1 which was well supported by Western blot analysis of H3K9Ac and H3K56Ac. Cellular protein levels of both Collagen type 1 and α-SMA were drastically increased by TGF-β1, whereas pre-treatment with GF considerably decreased the above alterations by reverse manners of SIRT1 in protein levels (Figure 7A,B). Accordingly, the Western blot analysis results and IHC analysis

well supported the effects of GF by regulations of SIRT1 with statistical significances (Figure 7C–F).

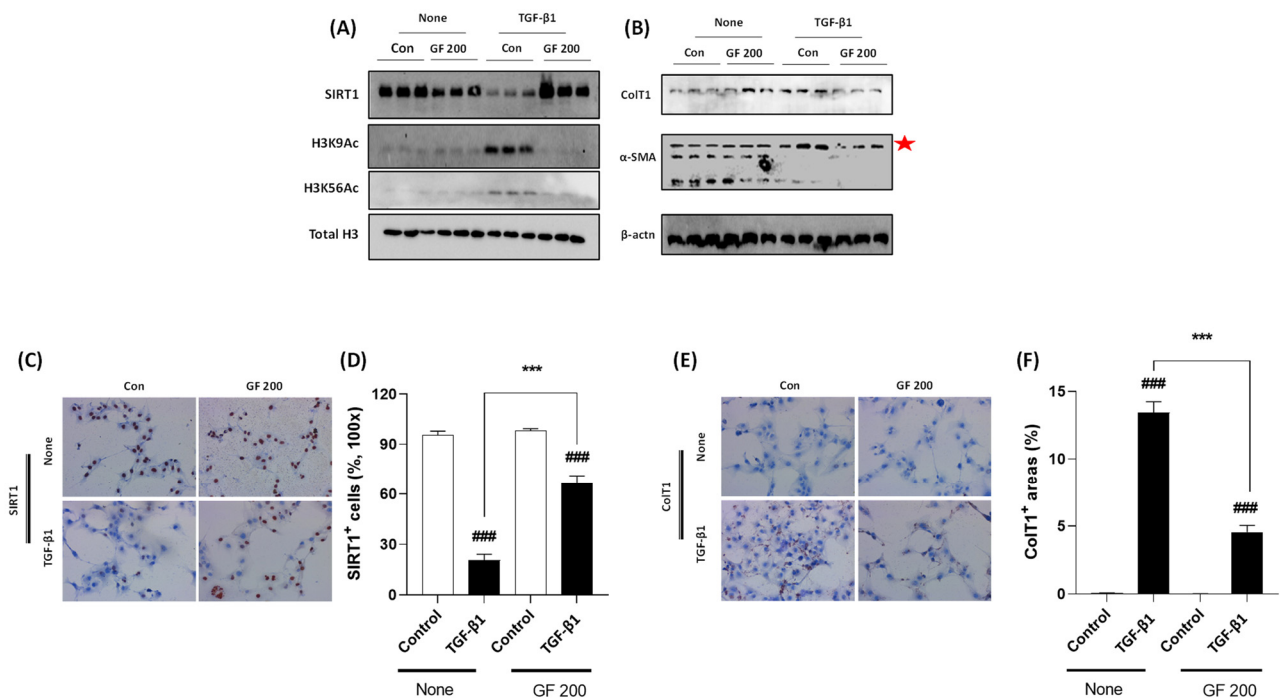


Figure 7. GF Alleviates TGF-β1-induced LX-2 Cell Activation via Enhancement of SIRT1. Western blot analysis in TGF-β1 treated LX-2 cells with or without GF. (A) Cellular protein levels of SIRT1, H3K9Ac, H3K56Ac, and Total H3. (B) Cellular protein levels of Collagen type 1, α-SMA, and β-actin. IHC analysis against SIRT1 (C) and its quantification analysis (D), and Collagen type 1 IHC (E) and its quantification analysis (F). Data were expressed mean ± SEM ($n = 3$ for Western blot analysis, $n = 4$ for IHC analysis). ### $p < 0.001$ for Control vs. TGF-β1 and *** $p < 0.001$ for None vs. GF 200. IHC images were captured by microscope condition (100× magnifications).

4. Discussion

Liver fibrosis is a process of wound and healing under the pathological status of chronic liver diseases. In liver fibrosis, the HSCs are well known to target cell type in the liver tissue to decide progression the next step of liver disease called liver cirrhosis or reversible to the non-pathological status of liver diseases [8,15]; however, there is no therapeutics to cure the liver fibrosis globally till nowadays. Thus, we aimed to investigate to develop medicine to treat liver fibrosis based on the natural plant, GF, especially [16] (Figure 1E–H), but didn't significantly recover in general physiological outcomes (Figure 1A–D).

Accumulated documents well displayed that TAA is a toxic agent to induce liver diseases via abnormal modulations of liver detoxification enzymes which can evoke oxidative stress-induced liver tissue damage and progress severe stages of liver diseases, called liver fibrosis and cirrhosis [17–19]. Thus, we addressed the effects of GF on the TAA-injected hepatic tissue oxidation. As expected, GF not only led to decreases of 4-HNE formations, serum and hepatic tissue levels of MDA, and serum MPO activities (Figure 2A–E) but also prevented hepatic endogenous antioxidants depletions such as SOD and GPx-1/2, respectively (Figure 2F,G). Additionally, chronic liver inflammation is invariably connected to liver fibrosis [20,21], and we partially proved the anti-inflammatory activities of GF against TAA-induced liver tissues. As shown in Figure 3A,B, the numbers of Kupffer cells in the hepatic tissue were considerably decreased by GF and pro-inflammatory such as IL-1β and TNF-α which are mainly activated by NF-κB in activated Kupffer cells during hepatic inflammation (Figure 3C,D). Furthermore, proteins by pending of NF-κB signaling pathway were normalized by GF (Figure 3E,F). Our findings are well comprised of the

representative pathophysiological status of hepatic inflammation by TAA-induced hepatic liver injury [22,23] and sufficient to support anti-hepatic inflammation effects on liver fibrosis by attenuations of pro-inflammatory cytokines as well as Kupffer cells activation related molecules (Figure 3A–F).

As we above mentioned, finally our mice were led to liver fibrosis conditions that mean excessive accumulation of ECMs proteins including predominantly fibrillar Collagen type 1 or Collagen type 3, and α -SMA, respectively [2,15]. Thus, we next investigated that the effects of GF on the modulations of activated HSCs in the hepatic tissue. Regarding liver fibrosis, our first finding which is IF analysis against HSCs by staining of HSCs were well corresponded to the GF effects by reducing their numbers in liver tissues (Supplementary Figure S3). Next, we further confirmed that anti-hepatofibrotic effects of GF are mainly attributed to alleviations of the huge amount of ECMs accumulation in liver tissues by evidence of both Masson's trichrome and Sirius Red stains (Figure 4A,B,F,G). These results are well supported by degradations of ECMs including α -SMA, Collagen type 1, and Collagen type 3, respectively (Figure 4C–E,H–J). Hepatic protein levels of TGF- β 1, known for pro-fibrogenic cytokine to promote HSCs activation or proliferation were drastically normalized by GF and other proteins such as TIMP-1, MMP-1, and MMP-13 which are known as ECMs promoters or degradations as responses of liver fibrosis [24,25]. Previous studies well reported that bile duct cells proliferation or ductular reactions in the liver tissue by TAA-induced liver fibrosis model [26]; however, in the present study ductular reactions in hepatic tissues were not affected by treatment with either TAA or GF (Supplementary Figure S4).

Liver fibrosis is normally comprehended by complicated events from various liver tissue-specific cell types including hepatocyte, Kupffer cells, and HSCs, respectively. Therefore, it is needed to understand the whole liver tissue events with specific molecular signaling transduction pathways. On the other hand, SIRT1 that is an epigenetic regulator well known to NAD⁺-dependent histone deacetylase is deeply implicated in liver diseases by modulations of redox status, inflammation, and cell death, respectively [27–31]; however, its roles in liver fibrosis is not clearly studied yet. Thus, we focused on our liver tissues by application of Western blot analysis and obtained that GF apparently inhibited H3K9Ac by blocking SIRT1 depletion in the liver protein levels (Figure 5A,C). As a partnership with SIRT1, AMPK is applied to regulate energy metabolism especially various energy homeostasis imbalances provoked pathological conditions [32]. This signaling pathway is a crucial factor in the approaches of various liver diseases [33–35]. The up-stream molecule of AMPK α , which is known to LKB1 is deeply associated with liver inflammation and metabolism [36,37]. According to our expectation, GF not only drastically increase AMPK α in liver protein levels, but also normalized hepatic protein levels of AMPK/SIRT1 signaling related or target molecules including NOX2, p47^{phox}, Nrf2, and HO-1, which mainly belong to liver tissue oxidation were significantly normalized by GF, especially respectively (Figure 5A,C).

Since we revealed that GF showed its pharmacological properties via regulation of hepatic SIRT1 and its related proteins, we further validated its pharmacological functions of GF in liver cell type-specific manners using HepG2 cells and LX-2 cells which are well corresponded to the hepatocytes and HSCs, respectively. First, we verified chronic oxidative stress depleted hepatocyte cellular levels of SIRT1 in H₂O₂ incubation HepG2 cells of 24 h experiment, not 6 h by applications of Western blot analysis and IHC analysis ($p < 0.001$ in Figure 6A,B,D,E). The IHC against 4-HNE analysis well supported the above results ($p < 0.001$ in Figure 6C,E). Pre-treatment with GF with various doses significantly prevented the depletion of SIRT1 in cellular protein levels of the chronic exposure against H₂O₂ condition ($p < 0.001$). Moreover, GF could block oxidative stress by the suppression of 4-HNE ($p < 0.001$). Along with this finding, the cell death signals were also normalized by GF by relieving apoptosis-related proteins, especially cytochrome *c* ($p < 0.001$ in Supplementary Figure S5A–D). In the case of HSCs, we can explain GF efficiently worked decreases of

ECMs including Collagen type 1, 3, and α -SMA by prevention of SIRT1 deteriorations in TGF- β 1 treated activated HSCs ($p < 0.001$ in Figure 7A–F and Supplementary Figure S6).

Previous studies well reported that geniposide which is an active compound from GF in various liver diseases especially NASH using pre-clinical in vivo models [38,39] and it also exerted to inhibit activations of HSCs [40], respectively. Pathophysiological progression of liver fibrosis, HSCs are the main target of advance this disease or reversely regression to the normal status [41]. Furthermore, GF also exerted antioxidant effects against ischemia/reperfusion in liver tissue of mice model [42] and alcoholic liver injury.

Unfortunately, till nowadays, there is no therapeutic access to treat liver fibrosis in the clinical area, so it is urgently sounded to develop efficacy guaranteed drugs based on the explanations of underlying mechanisms. Based on the accumulations of numerous clinical practice experiences, there are many possible candidates using herbal drugs to treat liver fibrosis [43–45]. Additionally, it is also needed to consider a possible mechanism to treat liver fibrosis based on the clear molecular levels of interactions. According to this, we focused on the well-known epigenetic regulator, SIRT1, which is histone deacetylase targeted to HSCs activation, hepatocyte oxidation, and inflammation, respectively [46,47].

In the present manuscript, we proved GF exerted to attenuate hepatic fibrosis against TAA-induced mice model by reduction of hepatocyte oxidation, amelioration of hepatic inflammation, decreases of ECM deposition through the liver tissue during fibrosis progression. Regarding the pharmacological effects of GF, we can conclude its actions as follows; (1) GF showed strong antioxidant effects by enhancement of endogenous antioxidant components in the liver tissue especially recoveries of SOD and GPx. (2) GF could regulate Kupffer cell activation and their numbers by diminishing pro-inflammatory cytokines. (3) GF strongly led to inactivate HSCs activation by evidence of amelioration of ECM resolutions and pro-fibrogenic cytokines during liver fibrosis. The corresponded mechanisms for the above properties of GF may regulate AMPK/SIRT1 signaling pathway in hepatocytes and HSCs, especially focusing on the beneficial effects of SIRT1 in both cell types.

Liver fibrosis is very a critical stage in the progression, which can decide to reserve normal stage or its advanced pathological stage such as liver cirrhosis or HCC, respectively. Nevertheless many trials to develop anti-hepatofibrosis therapeutics, there is no effective way existed in the world. From our study, we believe that GF would be one of the potential drug candidates to care for liver fibrosis. Therefore, further studies would be acquired to prove the safety and toxicity for clinical uses in the upcoming future.

Supplementary Materials: The following data are available online at <https://www.mdpi.com/article/10.3390/antiox10111837/s1>, Figure S1: Chemical composition analysis of Geniposide; Figure S2: Experimental scheme for animal experiment; Figure S3: Representative immunofluorescence image against Desmin; Figure S4: Representative images of bile duct reactions; Figure S5: Effects of Gardeniae Fructus against hepatocyte oxidation-induced cellular apoptosis; Figure S6: Effects of Gardeniae Fructus against LX-2 cell activation; Figure S7: Antibody lists for Western blot analysis; Figure S8: Antibody lists for Immunohistochemistry and immunofluorescence analysis.

Author Contributions: Writing—original draft, Writing—review & editing, M.-R.S.; investigation, J.M.; methodology, J.-W.N. and H.C.; conceptualization, J.A.L. and M.K.; Resources, Y.-J.M.; formal analysis, M.O. and S.L.; funding acquisition and supervision, S.-S.R. All authors have read and agreed to the published version of the manuscript.

Funding: This work was supported by the National Research Foundation of Korea (NRF) grant funded by the Korea government (MSIT) (No.2018R1A5A2025272).

Institutional Review Board Statement: The animal protocol used in this study was reviewed and approved by Daegu Haany University-Institutional Animal Care and Use Committee (approval no. DHU2021-012).

Informed Consent Statement: Not applicable.

Data Availability Statement: The data presented in this study are available on request from the corresponding author.

Conflicts of Interest: The authors declare no conflict of interest.

References

- Davis, J.P.E.; Caldwell, S.H. Healing gone wrong: Convergence of hemostatic pathways and liver fibrosis? *Clin. Sci. Lond.* **2020**, *134*, 2189–2201. [\[CrossRef\]](#)
- Bataller, R.; Brenner, D.A. Liver fibrosis. *J. Clin. Investig.* **2005**, *115*, 209–218. [\[CrossRef\]](#)
- Peng, R.; Wang, S.; Wang, R.; Wang, Y.; Wu, Y.; Yuan, Y. Antifibrotic effects of tanshinol in experimental hepatic fibrosis by targeting PI3K/AKT/mTOR/p70S6K1 signaling pathways. *Discov. Med.* **2017**, *23*, 81–94.
- Toosi, A.E. Liver Fibrosis: Causes and Methods of Assessment, a Review. *Rom. J. Intern. Med.* **2015**, *53*, 304–314. [\[CrossRef\]](#)
- Martinez, A.K.; Maroni, L.; Marzioni, M.; Ahmed, S.T.; Milad, M.; Ray, D.; Alpini, G.; Glaser, S.S. Mouse models of liver fibrosis mimic human liver fibrosis of different etiologies. *Curr. Pathobiol. Rep.* **2014**, *2*, 143–153. [\[CrossRef\]](#) [\[PubMed\]](#)
- Seo, H.Y.; Lee, S.H.; Lee, J.H.; Kang, Y.N.; Choi, Y.K.; Hwang, J.S.; Park, K.G.; Jang, B.K.; Kim, M.K. Clusterin Attenuates Hepatic Fibrosis by Inhibiting Hepatic Stellate Cell Activation and Downregulating the Smad3 Signaling Pathway. *Cells* **2019**, *8*, 1442. [\[CrossRef\]](#) [\[PubMed\]](#)
- Baiocchi, A.; Montaldo, C.; Conigliaro, A.; Grimaldi, A.; Correani, V.; Mura, F.; Ciccocanti, F.; Rotiroti, N.; Brenna, A.; Montalbano, M.; et al. Extracellular Matrix Molecular Remodeling in Human Liver Fibrosis Evolution. *PLoS ONE* **2016**, *11*, e0151736. [\[CrossRef\]](#)
- Higashi, T.; Friedman, S.L.; Hoshida, Y. Hepatic stellate cells as key target in liver fibrosis. *Adv. Drug Deliv. Rev.* **2017**, *121*, 27–42. [\[CrossRef\]](#) [\[PubMed\]](#)
- Chen, L.; Li, M.; Yang, Z.; Tao, W.; Wang, P.; Tian, X.; Li, X.; Wang, W. Gardenia jasminoides Ellis: Ethnopharmacology, phytochemistry, and pharmacological and industrial applications of an important traditional Chinese medicine. *J. Ethnopharmacol.* **2020**, *257*, 112829. [\[CrossRef\]](#)
- Ma, Z.G.; Kong, C.Y.; Song, P.; Zhang, X.; Yuan, Y.P.; Tang, Q.Z. Geniposide Protects against Obesity-Related Cardiac Injury through AMPK α - and Sirt1-Dependent Mechanisms. *Oxid. Med. Cell Longev.* **2018**, *2018*, 6053727. [\[CrossRef\]](#)
- He, T.; Shen, H.; Zhu, J.; Zhu, Y.; He, Y.; Li, Z.; Lu, H. Geniposide attenuates cadmium-induced oxidative stress injury via Nrf2 signaling in osteoblasts. *Mol. Med. Rep.* **2019**, *20*, 1499–1508. [\[CrossRef\]](#) [\[PubMed\]](#)
- Gillessen, A.; Schmidt, H.H. Silymarin as Supportive Treatment in Liver Diseases: A Narrative Review. *Adv. Ther.* **2020**, *37*, 1279–1301. [\[CrossRef\]](#)
- Mihara, M.; Uchiyama, M. Determination of malonaldehyde precursor in tissues by thiobarbituric acid test. *Anal. Biochem.* **1978**, *86*, 271–278. [\[CrossRef\]](#) [\[PubMed\]](#)
- Shin, M.-R.; Kim, M.J.; Park, H.J.; Han, J.G.; Roh, S.S. Beneficial effect of *Taraxacum coreanum* Nakai via the Activation of LKB1-AMPK Signaling Pathway on Obesity. *Evid. Based Complement. Alternat. Med.* **2021**, *2021*, 6655599. [\[CrossRef\]](#) [\[PubMed\]](#)
- Tsushima, T.; Friedman, S.L. Mechanisms of hepatic stellate cell activation. *Nat. Rev. Gastroenterol. Hepatol.* **2017**, *14*, 397–411. [\[CrossRef\]](#)
- Roehlen, N.; Crouch, E.; Baumert, T.F. Liver Fibrosis: Mechanistic Concepts and Therapeutic Perspectives. *Cells* **2020**, *9*, 875. [\[CrossRef\]](#)
- Low, T.Y.; Leow, C.K.; Salto-Tellez, M.; Chung, M.C. A proteomic analysis of thioacetamide-induced hepatotoxicity and cirrhosis in rat livers. *Proteomics* **2004**, *4*, 3960–3974. [\[CrossRef\]](#)
- Wallace, M.C.; Hamesch, K.; Lunova, M.; Kim, Y.; Weiskirchen, R.; Strnad, P.; Friedman, S.L. Standard operating procedures in experimental liver research: Thioacetamide model in mice and rats. *Lab. Anim.* **2015**, *49*, 21–29. [\[CrossRef\]](#) [\[PubMed\]](#)
- El Awdan, S.A.; Abdel Rahman, R.F.; Ibrahim, H.M.; Hegazy, R.R.; El Marasy, S.A.; Badawi, M.; Arbid, M.S. Regression of fibrosis by cilostazol in a rat model of thioacetamide-induced liver fibrosis: Up regulation of hepatic cAMP, and modulation of inflammatory, oxidative stress and apoptotic biomarkers. *PLoS ONE* **2019**, *14*, e0216301. [\[CrossRef\]](#)
- Campana, L.; Iredale, J.P. Regression of Liver Fibrosis. *Semin. Liver Dis.* **2017**, *37*, 1–10. [\[CrossRef\]](#)
- Koyama, Y.; Brenner, D.A. Liver inflammation and fibrosis. *J. Clin. Investig.* **2017**, *127*, 55–64. [\[CrossRef\]](#)
- Lin, Y.Y.; Hu, C.T.; Sun, D.S.; Lien, T.S.; Chang, H.H. Thioacetamide-induced liver damage and thrombocytopenia is associated with induction of antiplatelet autoantibody in mice. *Sci. Rep.* **2019**, *9*, 1–11. [\[CrossRef\]](#) [\[PubMed\]](#)
- Matsumoto, T.; Shimizu, T.; Nishijima, N.; Ikeda, A.; Eso, Y.; Matsumoto, Y.; Chiba, T.; Marusawa, H. Hepatic inflammation facilitates transcription-associated mutagenesis via AID activity and enhances liver tumorigenesis. *Carcinogenesis* **2015**, *36*, 904–913. [\[CrossRef\]](#) [\[PubMed\]](#)
- Hemmann, S.; Graf, J.; Roderfeld, M.; Roeb, E. Expression of MMPs and TIMPs in liver fibrosis—A systematic review with special emphasis on anti-fibrotic strategies. *J. Hepatol.* **2007**, *46*, 955–975. [\[CrossRef\]](#) [\[PubMed\]](#)
- Park, S.Y.; Shin, H.W.; Lee, K.B.; Lee, M.J.; Jang, J.J. Differential expression of matrix metalloproteinases and tissue inhibitors of metalloproteinases in thioacetamide-induced chronic liver injury. *J. Korean Med. Sci.* **2010**, *25*, 570–576. [\[CrossRef\]](#)
- Kamimoto, K.; Kaneko, K.; Kok, C.Y.; Okada, H.; Miyajima, A.; Itoh, T. Heterogeneity and stochastic growth regulation of biliary epithelial cells dictate dynamic epithelial tissue remodeling. *Elife* **2016**, *5*, e15034. [\[CrossRef\]](#)

27. Cao, Y.; Xue, Y.; Xue, L.; Jiang, X.; Wang, X.; Zhang, Z.; Yang, J.; Lu, J.; Zhang, C.; Wang, W.; et al. Hepatic menin recruits SIRT1 to control liver steatosis through histone deacetylation. *J. Hepatol.* **2013**, *59*, 1299–1306. [[CrossRef](#)]
28. Hart, R.A.; Diamandakis, V.; El-Khoury, G.; Buckwalter, J.A. A stress fracture of the scapular body in a child. *Iowa Orthop. J.* **1995**, *15*, 228–232.
29. Hisahara, S.; Chiba, S.; Matsumoto, H.; Tanno, M.; Yagi, H.; Shimohama, S.; Sato, M.; Horio, Y. Histone deacetylase SIRT1 modulates neuronal differentiation by its nuclear translocation. *Proc. Natl. Acad. Sci. USA* **2008**, *105*, 15599–15604. [[CrossRef](#)] [[PubMed](#)]
30. Hwang, J.W.; Yao, H.; Caito, S.; Sundar, I.K.; Rahman, I. Redox regulation of SIRT1 in inflammation and cellular senescence. *Free Radic. Biol. Med.* **2013**, *61*, 95–110. [[CrossRef](#)]
31. Tanno, M.; Sakamoto, J.; Miura, T.; Shimamoto, K.; Horio, Y. Nucleocytoplasmic shuttling of the NAD⁺-dependent histone deacetylase SIRT1. *J. Biol. Chem.* **2007**, *282*, 6823–6832. [[CrossRef](#)] [[PubMed](#)]
32. Ruderman, N.B.; Xu, X.J.; Nelson, L.; Cacicedo, J.M.; Saha, A.K.; Lan, F.; Ido, Y. AMPK and SIRT1: A long-standing partnership? *Am. J. Physiol. Endocrinol. Metab.* **2010**, *298*, E751–E760. [[CrossRef](#)] [[PubMed](#)]
33. Li, S.; Qian, Q.; Ying, N.; Lai, J.; Feng, L.; Zheng, S.; Jiang, F.; Song, Q.; Chai, H.; Dou, X. Activation of the AMPK-SIRT1 pathway contributes to protective effects of Salvianolic acid A against lipotoxicity in hepatocytes and NAFLD in mice. *Front. Pharmacol.* **2020**, *11*, 560905. [[CrossRef](#)] [[PubMed](#)]
34. Yang, Y.; Bai, T.; Yao, Y.L.; Zhang, D.Q.; Wu, Y.L.; Lian, L.H.; Nan, J.X. Upregulation of SIRT1-AMPK by thymoquinone in hepatic stellate cells ameliorates liver injury. *Toxicol. Lett.* **2016**, *262*, 80–91. [[CrossRef](#)]
35. Jiang, Z.; Zhou, J.; Zhou, D.; Zhu, Z.; Sun, L.; Nanji, A.A. The adiponectin-SIRT1-AMPK pathway in alcoholic fatty liver disease in the rat. *Alcohol. Clin. Exp. Res.* **2015**, *39*, 424–433. [[CrossRef](#)]
36. Chen, T.; Moore, T.M.; Ebbert, M.T.; McVey, N.L.; Madsen, S.R.; Hallowell, D.M.; Harris, A.M.; Char, R.E.; Mackay, R.P.; Hancock, C.R.; et al. Liver kinase B1 inhibits the expression of inflammation-related genes postcontraction in skeletal muscle. *J. Appl. Physiol.* **1985** *2016*, *120*, 876–888. [[CrossRef](#)]
37. Just, P.A.; Charawi, S.; Denis, R.G.P.; Savall, M.; Traore, M.; Foretz, M.; Bastu, S.; Magassa, S.; Senni, N.; Sohier, P.; et al. Lkb1 suppresses amino acid-driven gluconeogenesis in the liver. *Nat. Commun.* **2020**, *11*, 6127. [[CrossRef](#)]
38. Chen, C.; Xin, X.; Liu, Q.; Tian, H.J.; Peng, J.H.; Zhao, Y.; Hu, Y.Y.; Feng, Q. Geniposide and Chlorogenic Acid Combination Improves Non-Alcoholic Fatty Liver Disease Involving the Potent Suppression of Elevated Hepatic SCD-1. *Front. Pharmacol.* **2021**, *12*, 653641. [[CrossRef](#)]
39. Ma, T.; Huang, C.; Zong, G.; Zha, D.; Meng, X.; Li, J.; Tang, W. Hepatoprotective effects of geniposide in a rat model of nonalcoholic steatohepatitis. *J. Pharm. Pharmacol.* **2011**, *63*, 587–593. [[CrossRef](#)]
40. Lin, X.; Li, J.; Xing, Y.Q. Geniposide, a sonic hedgehog signaling inhibitor, inhibits the activation of hepatic stellate cell. *Int. Immunopharmacol.* **2019**, *72*, 330–338. [[CrossRef](#)]
41. Zhang, C.Y.; Yuan, W.G.; He, P.; Lei, J.H.; Wang, C.X. Liver fibrosis and hepatic stellate cells: Etiology, pathological hallmarks and therapeutic targets. *World J. Gastroenterol.* **2016**, *22*, 10512–10522. [[CrossRef](#)] [[PubMed](#)]
42. Kim, J.; Kim, H.Y.; Lee, S.M. Protective Effects of Geniposide and Genipin against Hepatic Ischemia/Reperfusion Injury in Mice. *Biomol. Ther. Seoul* **2013**, *21*, 132–137. [[CrossRef](#)]
43. Ge, H.; Wang, A.; Su, Y.; Yu, C.; Gao, L.; Li, Y. Ameliorative effects of Qingganjiuwei powder, a traditional Mongolian medicine, against CCl₄-induced liver fibrosis in rats. *J. Ethnopharmacol.* **2021**, *264*, 113226. [[CrossRef](#)]
44. Choi, M.J.; Zheng, H.M.; Kim, J.M.; Lee, K.W.; Park, Y.H.; Lee, D.H. Protective effects of *Centella asiatica* leaf extract on dimethylnitrosamine-induced liver injury in rats. *Mol. Med. Rep.* **2016**, *14*, 4521–4528. [[CrossRef](#)] [[PubMed](#)]
45. Li, M.Y.; Ryan, P.; Batey, R.G. Traditional Chinese medicine prevents inflammation in CCl₄-related liver injury in mice. *Am. J. Chin. Med.* **2003**, *31*, 119–127. [[CrossRef](#)]
46. Ramirez, T.; Li, Y.M.; Yin, S.; Xu, M.J.; Feng, D.; Zhou, Z.; Zang, M.; Mukhopadhyay, P.; Varga, Z.V.; Pacher, P.; et al. Aging aggravates alcoholic liver injury and fibrosis in mice by downregulating sirtuin 1 expression. *J. Hepatol.* **2017**, *66*, 601–609. [[CrossRef](#)] [[PubMed](#)]
47. Ramzy, M.M.; Abdelghany, H.M.; Zenhom, N.M.; El-Tahawy, N.F. Effect of histone deacetylase inhibitor on epithelial-mesenchymal transition of liver fibrosis. *IUBMB Life* **2018**, *70*, 511–518. [[CrossRef](#)] [[PubMed](#)]